AIAA JOURNAL
Vol. 31, No. 1, January 1993

Engineering Approach to the Prediction of Shock Patterns in Bounded High-Speed Flows

D. J. Azevedo* and Ching Shi Liu†
State University of New York at Buffalo, Amherst, New York 14260

A two-dimensional symmetric wedge configuration representative of a simple high-speed intake in steady flow was investigated. The analysis presented here is intended as an engineering approach for estimating certain features of the internal shock system. The primary interest here is the prediction of the size and location of the almost-normal shock wave that develops when the leading-edge shocks intersect at angles above a certain critical value that is less than the wedge detachment angle. The almost-normal shock wave is frequently referred to as the "Mach stem," Parametric studies enabled the sensitivity of the Mach stem height to various flowfield parameters to be examined, thus indicating how accurately these parameters must be measured in a given experiment. Results of these predictions were compared with those of a steady-flow experiment performed at nominal freestream Mach numbers from 2.8 to 5. The predicted stem heights were consistently lower than the mean experimental values, attributable both to experimental uncertainties and to certain simplifying assumptions used in the analysis. Modification of these assumptions to better represent the test environment improved the analytical results.

Nomenclature

A	= cross-sectional area
A_1	= inlet area of wedge configuration
A_t	= area at wedge trailing edge
e	= internal energy per unit mass
L	= wedge length parallel to upstream flow direction
M	= Mach number
$\dot{m}$	= mass flow rate
n	= unit normal vector
P	= distance between Mach stem and wedge trailing edge; also stagnation pressure
p	= static pressure
R	= gas constant, 287 J/kg K
T	= static temperature
V	= velocity
w	= length of wedge face
x	= horizontal distance, with origin at Mach stem
y	= vertical distance, with origin at symmetry plane
y_1	= distance between symmetry plane and wedge leading edge
y_m	= length of Mach stem
y_t	= distance between symmetry plane and wedge trailing edge
β	= acute angle of incident shock with respect to upstream flow direction
β_d	= shock angle associated with detachment of shock wave from a wedge
β_N	= von Neumann angle
β_s	= shock angle resulting in sonic flow behind the shock wave
β_{23}	= acute angle between the reflected shock wave and the flow vector behind the incident shock wave
γ	= ratio of specific heats
ϵ	= angle of the slipstream with respect to the upstream flow direction
θ	= wedge angle (or flow deflection angle due to the incident shock wave)
θ_{23}	= flow deflection angle due to reflected shock wave
μ	= Mach angle
ρ	= static density

Subscripts

1,2,3,4	= various regions of the Mach reflection flowfield
*	= conditions at a location where $M = 1$
0	= stagnation conditions

Introduction

CURRENT supersonic vehicle designs must cope with the presence of shock systems, whether they occur within the vehicle frame or about surfaces attached to the external shell. Figure 1a illustrates a shock system within a ramjet configuration. Obviously, the stagnation pressure losses due to the many shocks are of concern, particularly those associated with any normal shocks that might develop. If A_t is too small, the duct becomes too strong a diffuser and may act to "unstart" the flow, resulting in subsonic flow throughout. Goldberg and Hefner[1] presented a plot of the area ratio of the duct, A_1/At, vs the upstream Mach number that shows the ratios that lead to an unstart. One difficulty with their plot is that the stagnation pressure drop across the duct must be specified to find the correct limiting A_1/A_t value for a given freestream Mach number. Knowledge of the lengths associated with the Mach reflection shock system, however, enables one to compute some mass-weighted, overall stagnation pressure drop for the duct due solely to the internal shocks.[2] This, in turn, should improve a given vehicle design so that an unstart may be avoided. An additional point about the importance of length-scale predictions is that relatively high noise levels are produced in the subsonic region behind normal shock waves in otherwise supersonic flows.[3] Minimization of this subsonic "patch" and its acoustic contribution may be a factor in future vehicle designs.

Figure 1b also illustrates a typical interaction between an oblique shock and a bow wave of the type investigated by Edney.[4] High heat transfer to the blunt-body surface can occur in these situations, depending on both the strength of the incident shock and the location of impingement. A key

Received Nov. 27, 1991; revision received May 21, 1992; accepted for publication May 21, 1992.

*Graduate Student, Department of Mechanical and Aerospace Engineering; currently Senior Engineer, Pratt and Whitney, P.O. Box 109600, West Palm Beach, FL 33410. Member AIAA.

†Associate Professor, Department of Mechanical and Aerospace Engineering.

element of certain computational codes currently employed to predict such heating loads is the length scale X given in the figure. This length scale is believed by the authors to be analogous to the Mach stem observed in situations such as that shown in Fig. 1a, and in fact this is what led the authors to investigate the current problem. Empirical values are normally utilized, but it would be convenient if estimates of X could be developed solely from the known freestream conditions and body geometry.

To outline the problem more clearly, we present Fig. 2a, which depicts the steady-flow situation whereby a shock wave attached to a wedge reflects off a solid interface. Such a regular reflection (RR) is typically not specular, the reflected wave inclined at an angle (relative to the upstream flow) less than that of the incident shock wave. This RR pattern is the half-plane view of the symmetric wedge configuration shown in Fig. 2b.

As the wedge angles are increased, the regular reflection makes a transition to what is commonly known as Mach reflection (MR), named after Ernst Mach, who first reported the phenomenon in 1878. The MR pattern, illustrated in Fig. 3, is distinguished from RR by 1) the embedded subsonic region behind the almost-normal Mach stem and 2) the existence of a slipstream (dashed line) originating at the confluence of the three shocks and separating the supersonic flow in region 3 from the subsonic flow in region 4. The slipstream arises from the entropy difference in regions 3 and 4 and is frequently treated, in an inviscid sense, as a thin discontinuity at which the velocity vectors V_3 and V_4 are parallel (i.e., there is no mass flux across the slipstream) and on either side of which the static pressures are equal (stationary slipstream).

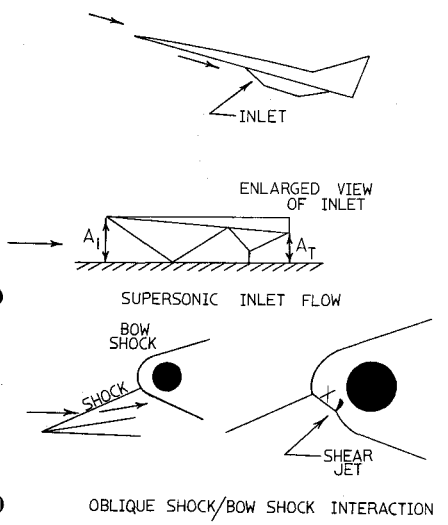

Fig. 1 Examples of Mach reflection in actual hypersonic flows.

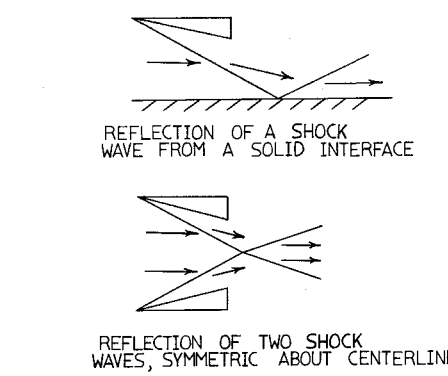

Fig. 2 Regular reflection of oblique shock waves in steady inviscid flows.

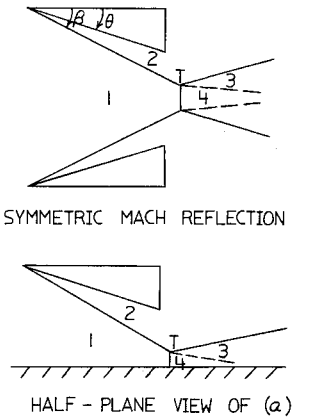

Fig. 3 Mach reflections in steady flow, assuming uniform flow in all regions.

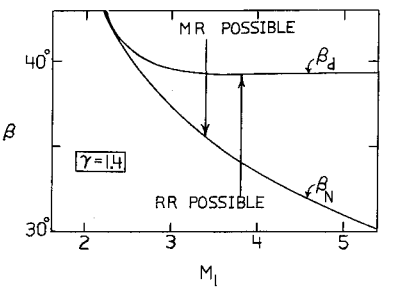

Fig. 4 Comparison of the shock angles used to denote transition from regular reflection with Mach reflection (after Ref. 10).

The Mach stem can be thought of as developing to insure a continuous transition from RR to MR. This "mechanical equilibrium" concept was originally suggested by von Neumann[5] and resurrected by Henderson and Lozzi.[6] (Ben-Dor[7] notes that, for fixed initial conditions and steady flow, there is no need to require a continuous pressure change during transition because no transition occurs. If a transition from RR→MR does occur, however, by varying the initial conditions, then he concludes that the mechanical equilibrium concept may be valid.) Thus, at transition, the pressure rise across the two oblique shocks (incident and reflected) just equals the pressure rise associated with a normal shock for the same upstream conditions. The minimum incident shock angle β_N at which this occurs is generally referred to as the von Neumann angle and is given by[8]

$$\cot^4\beta_N - \frac{[\gamma\mu^2(\xi+\mu^2)+(1-\xi)^2]}{(\xi+\mu^2)(1+\mu^2\xi)}\cot^2\beta_N - \frac{\gamma(\xi+\mu^2)}{(1+\mu^2\xi)^2} = 0 \quad (1)$$

where

$$\mu^2 = \frac{\gamma-1}{\gamma+1}$$

$$\xi = \frac{p_1}{p_2}$$

It is apparent that β_N depends only on the incident Mach number and the ratio of specific heats. A sufficiently high downstream pressure can, however, markedly decrease the RR→MR transition angle, as noted by Henderson and Lozzi.[9]

There is an alternate criterion, also proposed by von Neumann, termed the "detachment criterion." This identifies RR→MR as imminent when the incident shock angle β results in a reflected shock-wave angle that can no longer turn the flow parallel to the symmetry plane or inviscid wall. The reflection point is thus seen as becoming detached from the symmetry plane, with a normal shock connecting the reflec-

tion point to the symmetry plane to satisfy the boundary condition there. The difference $\beta_d - \beta_N$ (β_d is the incident shock angle associated with the "detached" reflected shock) increases as the upstream number M_1 increases above about 2.4, as shown in Fig. 4. The tests of Hornung and Robinson[10] essentially confirmed β_N as the correct transition criterion for steady flow. The angle β_d seems to be appropriate for those wedge flows defined as "pseudosteady"[11] (self-similar).

This paper is concerned with predicting the scale of the shock pattern for $\beta > \beta_N$ for a given wedge geometry. Although a unique solution for the steady-flow case is not claimed, it is desired to investigate whether a predictable pattern is possible that agrees with experimental observations. More specifically, the interest is in the Mach stem height variation with β, since this shock connects (in the symmetric wedge case) the two incident shocks and also forms the inlet area for what can be considered a subsonic nozzle (see region 4 in Fig. 3a). As will be seen, a sonic line can develop in region 4 if the downstream pressure is low enough. Thus, knowing the Mach stem height allows the length of the subsonic patch to be estimated, provided some model of the flow acceleration is specified. Of course, such a model would have to incorporate some mechanism for reconciling this flow acceleration with the requirement of "no mass flux" across the slipstream, mentioned earlier.

Another concern of this paper is the validity of the Rankine-Hugoniot (R-H) equations as a means for determining the local conditions at the confluence, or triple, point. Von Neumann had assumed straight shocks and uniform flow in each region about this triple point to develop a polynomial expression, Eq. (1), for β_N. Curle and Davies,[12] employing the same assumptions, presented an iterative solution of the R-H equations as a means for determining the shock angles and flow conditions at the triple point for $\beta > \beta_N$. These assumptions are strictly valid only in a vanishingly small region about the triple point T in Figs. 3a and 3b. Additionally, downstream conditions are assumed to have no effect on the local flowfield solution.

Only a handful of investigators have considered the influence that wedge geometry could have on the steady-state Mach reflection pattern. Sternberg[13] noted that the expansion fan centered at the wedge trailing edge could increase the scale of the shock pattern by displacing the Mach stem upstream, but he did not present any mechanism to explain this. Later experimental work by Henderson and Lozzi[9] showed that RR could be suppressed altogether for a given A_1/A_t ratio (Fig. 1a) by sufficiently increasing the downstream pressure.

The Hornung and Robinson[10] experiments, mentioned earlier, were performed with a symmetric wedge configuration. The downstream pressure was always low enough to avoid the unstart effects noted in Ref. 9. Wedge lengths were chosen so that the reflected shock would not pass too close to the wedge trailing edge, a condition observed[13] to produce the same result as a high downstream pressure, that is, an upstream displacement of the Mach stem and a subsequent reduction of the RR−MR transition angle.

The present work can be considered as an extension of the work of von Neumann[5] (and Curle and Davies[12]), in that the local conditions about the triple point will be assumed to hold over a *finite* region. This allows length scales in the flowfield (i.e., the shock structure) to be easily determined, with the restriction that downstream conditions do not influence the flowfield.

Model

The goal here is to develop some simple framework that will allow certain length scales in the Mach reflection flowfield to be determined. Since the Mach stem is physically tied to both the incident and reflected shocks, and to the slipstream, and forms the inlet area of the subsonic region, it is the primary length scale of interest. The approach taken is to solve for the Mach stem height and location in the duct using a control volume analysis. The geometry studied here is a symmetric two-dimensional wedge configuration. Symmetry allows the half-plane view to be employed in the following discussion. All of the physical phenomena included in the steady-flow situation are shown in Fig. 5. With reference to this diagram, our analysis is based on the following assumptions:

1) Upstream conditions alone are sufficient to determine the flow conditions about the point T.

2) The reflected shock angle β_{23} is a constant for given upstream conditions.

3) The Mach stem y_M is a normal shock.

4) The slipstream is inclined toward the symmetry plane, at a constant angle with respect to the symmetry plane. Thus, the static pressure on either side of the slipstream is the same, at all points along the slipstream.

5) The region behind the Mach stem, one of accelerating subsonic flow, can be treated with one-dimensional gas dynamics. The apparent contradiction with the previous assumption of equal static pressures on either side of the slipstream will be resolved in the discussion to follow.

6) The wedge is short enough that the reflected shock wave does not hit it.

7) The leading characteristic of the expansion wave, originating at the wedge trailing edge and refracted by the reflected shock wave, intersects the slipstream and defines the location of the sonic line in region 4. The downstream pressure is assumed low enough that a sonic line always forms.

The following discussion elaborates on each of these assumptions. Although some empirical justification is available, it will be made clear where more rigorous proof is needed. Indeed, one of the intentions of this simplified model was just that—to point out those aspects of the problem where further efforts should be concentrated.

Unpublished optical data from Hornung and Robinson's study,[10] made available to these authors by Hornung, verified (to within the measurement uncertainty) that the reflected shock angle β_{23} agrees with the triple-point solution of Curle and Davies.[12] [Two reflected shock angles are theoretically possible according to the R-H equations, but only one (weak solution) will allow the flow behind it to be supersonic, which is what is experimentally observed for Mach numbers above about 2.23 and low downstream pressures. Conversely, the strong solution is appropriate for the Mach stem solution.] A uniform flow assumption (i.e., assumptions 1 and 2 listed earlier) is therefore reasonable for regions 1, 2, and 3, with the conditions determinable from the upstream flow conditions.

As a first approximation, the Mach stem will be assumed to be a normal shock. This approximation was suggested by the triple-point solutions computed by the authors for a wide range of freestream flows. These solutions indicated that the angle of the Mach stem at the triple point is always very nearly 90 deg (with respect to the symmetry plane) for $\beta > \beta_N$. The use of a normal shock is convenient in that the solution for the shock height may then be used to determine its location,

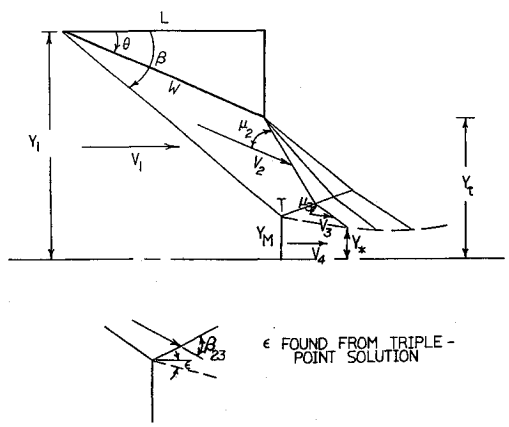

Fig. 5 Sketch illustrating some of the nomenclature to be used.

relative to the wedge trailing edge, by considering the geometric relation between the incident and Mach shocks [see Eq. (10)]. Also, since the slipstream angle ϵ is generally less than 10 deg for incident shock angles close to the von Neumann angle, a one-dimensional flow approximation will be used to relate the stem height y_M and the sonic throat height y_*. As noted previously, the angled slipstream and assumed nonmixing of the adjacent regions 3 and 4 result in a subsonic flow acceleration. An isentropic, one-dimensional flow model agreed well with data obtained in the relevant experimental work of both Chow and Addy,[14] and Back and Cuffel,[15] and thus was employed in the present study.

In general, some slipstream curvature is to be expected because of the favorable pressure gradient in region 4 and the influence of the expansion fan centered at the wedge trailing edge (see Fig. 5). Since the reflection pattern is a steady one, it appears that the condition $p_3 = p_4$ is satisfied. It is suggested, though, that p_4 be defined as $p_4(y)$, such that $p_3 = p_4(y)$ at the y value corresponding to the slipstream. Thus, the pressure condition is here relaxed to $p_3 = p_{4\text{avg}}$, where $p_{4\text{avg}}$ is represented by

$$p_{4\text{avg}} = \frac{\int_0^{y_{\max}} p_4 \, dy}{\int_0^{y_{\max}} dy} \tag{2}$$

where $y_{\max}$ represents the height above the symmetry plane at which the slipstream is encountered at each axial location. This approach is suggested as a means by which the nonuniform region in region 4 can be made consistent with the requirement of equal static pressure on both sides of the slipstream.

Thus, whereas von Neumann's original three-shock theory required $p_3 = p_4$ *at* the confluence point, the condition $p_3 = p_{4\text{avg}}$ is proposed for regions *away from* the confluence point. There is some precedent for relaxing the pressure condition in the work of Skews.[16]

An *inviscid* mechanism allowing p_4 to vary in the manner suggested relates to the slipstream curvature (Fig. 5). The static pressure increases from the symmetry plane to the slipstream so that $p_3 = p_4$ at the slipstream. Moreover, the curvature can be made consistent with aforementioned assumption 4 if one is willing to accept ϵ as some *effective* slipstream angle different from that of the triple-point solution. Note that such local curvature is assumed not to invalidate the uniform-flow assumption in region 3.

The presence of the shear layer originating at the confluence point allows one to also consider a *viscous* mechanism for the relaxed pressure condition, that is, the growth of the shear layer on both sides of the slipstream. By computing the displacement thickness associated with the growth in each region, Ben-Dor[17] found that the resulting slipstream angle differed from that of inviscid theory (e.g., triple-point solution). (Note that the displacement thickness for region 4 will be negative, whereas for region 3 it is positive.) It is expected that the viscous contribution will be small (i.e., that the slipstream angles are only slightly altered from those computed using three-shock theory) since the experimental RR→MR transition angles of Hornung and Robinson[10] agreed closely with inviscid theory.

Assumption 6 was imposed simply to allow the equations (to be presented in the next section) to be easily manipulated. There appears to be no fundamental reason why the use of a longer wedge, with an increased number of internal shocks, cannot be investigated with the approach described in this paper. This point will be raised again after the governing equations have been presented.

If no expansion waves were present, the flow in region 4 would become parallel to the wall, as would the slipstream, and the adjacent regions would merge smoothly at some downstream location. The role of the expansion, as described by Hornung,[11] is to bend the slipstream away from the wall, creating a sonic line (throat) in the subsonic region, provided the downstream pressure is sufficiently low. Assumption 7 defines the location of the sonic line in region 4 to be the axial location where the expansion wave's leading characteristic and the slipstream intersect. This argument may be strengthened by realizing that the leading characteristic of the expansion wave is a Mach line. Recall that a one-dimensional flow acceleration has been assumed here for the subsonic region, which necessarily results in a planar sonic line downstream of the normal Mach stem. Since the component of the Mach number normal to a Mach line is unity, as is the Mach number at the sonic throat, the sonic line can be considered to be an extension of the leading characteristic of the expansion. Although this argument alone is by no means conclusive, it is considered strong enough to justify its use here. This assumption also allows the governing equations to be made analytically tractable.

A control volume may now be defined (Fig. 6), across which the usual inviscid conversation equations can be applied. By assuming all discontinuities to be straight, the integral relations reduce to algebraic ones, greatly simplifying the analysis. The slipstream is inclined at some constant angle that, in general, differs from that given by the triple-point solution, as discussed previously.

The lettering delineates the various segments of the control surface. Lengths y_1, y_M, and y_* represent, respectively, the inlet, Mach stem, and throat heights. Segments GF and FE represent the leading characteristic of the trailing-edge expansion fan, with FE representing that portion refracted by the reflected shock wave TF. The slipstream is given by TE, and the symbol P represents the distance between the Mach stem and the wedge trailing edge. Positive values ($P > 0$) imply that the stem is positioned downstream of the trailing edge, and negative values ($P < 0$) result when the stem resides upstream of the trailing edge.

It is convenient to consider such a control volume, since the choice of control surface elements at the downstream end avoids the need to consider the upstream propagation of any disturbances downstream of the line GFE. Again, one must assume that the far downstream pressure is low enough that formation of a throat is possible.

The formation of the leading characteristic of the expansion wave is dependent only on the supersonic flow ahead of it. This is expressed mathematically as $\sin(\mu_2) = 1/M_2$, where the Mach angle μ_2 is that between the velocity vector V_2 ahead of the characteristic and the characteristic line GF. A similar mathematical relationship holds between the local angle of the refracted portion of the characteristic and the Mach number M_3, i.e., $\sin(\mu_3) = 1/M_3$. The assumption of straight characteristics is employed to avoid complicating the equations, thus allowing an analytical solution.

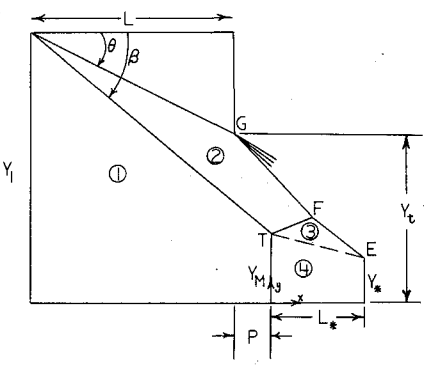

Fig. 6 Control volume.

Equations

The inviscid conservation equations, written in integral form, are

Continuity:

$$\int_{cs} \rho V \cdot dA = 0 \tag{3}$$

X momentum:

$$-\int_{cs} (pn \cdot dA)_x = \int_{cs} V_x(\rho V \cdot dA) \tag{4}$$

Y momentum:

$$-\int_{cs} P(V \cdot dA)_y = \int_{cs} V_y(\rho V \cdot dA) \tag{5}$$

Energy:

$$-\int_{cs} P(V \cdot dA) = \int_{cs} (e + V^2/2)(\rho V \cdot dA) \tag{6}$$

where

$$e = \left(\frac{1}{\gamma - 1}\right)\left(\frac{p}{\rho}\right)$$

and where variables in bold type denote vectors, and cs stands for control surface.

Since we are considering the flow to be inviscid and adiabatic, the energy equation is redundant. This is seen more clearly by rearranging Eq. (6) to get

$$\int_{cs}\left[\frac{p}{\rho}\left(\frac{\gamma}{\gamma - 1}\right) + \frac{1}{2}V^2\right](\rho V \cdot dA) = 0 \tag{6'}$$

where $(p/\rho)(\gamma/\gamma - 1) + \frac{1}{2}V^2 = H_0$, the stagnation enthalpy, which is a constant for the flowfield under consideration. Thus, Eq. (6) is identical to Eq. (3).

We now replace the area vectors by the various control surface elements. Using the length L as a normalizing parameter, Eqs. (3–6) become

Continuity:

$$\rho_1 V_1 \frac{y_1}{L} = \rho_2(V_2 \sin \mu_2)\frac{GF}{L} + \rho_3(V_3 \sin \mu_3)\frac{FE}{L} + \rho_* V_* \frac{y_*}{L} \tag{3'}$$

X momentum:

$$p_1\frac{y_1}{L} - p_2 \tan \theta - p_2' \sin(\mu_2 + \theta)\frac{GF}{L} + p_3' \sin(\mu_3 + \epsilon)\frac{FE}{L} - p_*\frac{y_*}{L} = (\rho_2 V_2 \sin \mu_2)(V_2 \cos \theta)\frac{GF}{L} + (\rho_3 V_3 \sin \mu_3)(V_3 \cos \epsilon)\frac{FE}{L} + p_* V_*^2\frac{y_*}{L} - \rho_1 V_1^2\frac{y_1}{L} \tag{4'}$$

Y momentum:

$$p_1\left(1 + \frac{P}{L}\right) + p_4\frac{L_*}{L} - p_2 - p_2' \cos(\mu_2 + \theta)\frac{GF}{L} - p_3' \cos(\mu_3 + \epsilon)\frac{FE}{L} = -(V_2 \sin \theta)(\rho_2 V_2 \sin \mu_2)\frac{GF}{L} - (V_3 \sin \epsilon)(\rho_3 V_3 \sin \mu_3)\frac{FE}{L} \tag{5'}$$

In these equations, the primed (′) quantities designate the flow state on the downstream side of the leading characteristic of the expansion fan. The starred (*) quantities denote conditions at the sonic throat.

The following simplifications may now be made:

1) The pressures on either side (upstream or downstream) of the expansion fan's leading characteristic are similar enough that one can assume $p_2 = p_2'$ and $p_3 = p_3'$.

2) The starred conditions result from an isentropic one-dimensional flow acceleration to sonic conditions, with the acceleration originating behind the normal Mach stem.

3) $p_3 = p_{4\text{avg}}$

4) $\gamma = \text{const}$ (for the results to be presented, γ was taken to be 1.4).

The final forms of the equations are given next:

Continuity:

$$\frac{y_1}{L} = \left[\frac{\sin \beta}{M_2 \sin(\beta - \theta)}\right]\frac{GF}{L} + \left[\frac{\sin \beta \sin \beta_{23}}{M_3 \sin(\beta - \theta)\sin(\beta_{23} - \theta_{23})}\right]\frac{FE}{L} + (f_0)\frac{y_*}{L} \tag{3''}$$

X momentum:

$$\frac{y_1}{L} - \frac{p_2}{p_1}\frac{\tan \theta}{1 + \gamma M_1^2} = \left\{\frac{p_2}{p_1}\frac{[\sin(\mu_2 + \theta) + \gamma M_2 \cos \theta]}{1 + \gamma M_1^2}\right\}\frac{GF}{L} + \left\{\frac{p_3}{p_1}\frac{[\sin(\mu_3 + \epsilon) + \gamma M_3 \cos \epsilon]}{1 + \gamma M_1^2}\right\}\frac{FE}{L} + \left[\frac{p_*}{p_1}\left(\frac{\gamma + 1}{1 + \gamma M_1^2}\right)\right]\frac{y_*}{L} \tag{4''}$$

Y momentum:

$$1 - \frac{p_2}{p_1} = \left\{\frac{p_2}{p_1}[\cos(\mu_2 + \theta) - \gamma M_2 \sin \theta]\right\}\frac{GF}{L} + \left\{\frac{p_3}{p_1}[\cos(\mu_3 + \epsilon) - \gamma M_3 \sin \epsilon]\right\}\frac{FE}{L} - \left[\frac{p_3}{p_1}\right]\frac{L_*}{L} - \frac{P}{L} \tag{5''}$$

where

$$f_0 = \frac{P_{0*}}{P_{04}} M_* \frac{[2\gamma M_1^2 - (\gamma - 1)]^{(-1/\gamma - 1)}}{[(\gamma - 1)M_1^2 + 2]^{1/2}}[(\gamma + 1)M_1^2]^{[\gamma - 1/2(\gamma - 1)]} \tag{7}$$

and where P_{04} = stagnation pressure behind Mach stem and

$$\frac{P_{0*}}{P_{04}} = 1$$

where $M_* = 1$ for isentropic acceleration to sonic condition.

It is seen that the coefficients of the defined, normalized length scales (i.e., the elements of the control surface) are constant for given steady-flow freestream conditions and wedge geometry. These coefficients were computed using the Curle and Davies[12] triple-point solution algorithm. Now two more equations are still needed to solve for the five unknowns (GF/L, FE/L, y_*/L, L_*/L, and P/L). These equations are geometric relations between L_*/L and the other length scales:

$$\frac{L_*}{L} = \cos(\mu_2 + \theta)\frac{GF}{L} + \cos(\mu_3 + \epsilon)\frac{FE}{L} - \frac{P}{L} \tag{8}$$

$$\frac{y_*}{L} = \frac{y_t}{L} - \sin(\mu_2 + \theta)\frac{GF}{L} - \sin(\mu_3 + \epsilon)\frac{FE}{L} \tag{9}$$

Once P/L is known, the Mach stem height can be obtained from

$$\frac{P}{L} = \frac{[(y_t/L) - (y_M/L)] + (\tan \theta - \tan \beta)}{\tan \beta} \tag{10}$$

Equations (3″-5″), (8), and (9) represent five equations to which a matrix solution technique will be applied. Although the matrix analysis is a linear one, implying the solution is unique, it is recognized that this may not be true for all situations.[17]

The matrix to be solved looks as follows:

$$\begin{vmatrix} A_1 & B_1 & C_1 & D_1 & E_1 \\ A_2 & B_2 & C_2 & D_2 & E_2 \\ A_3 & B_3 & C_3 & D_3 & E_3 \\ A_4 & B_4 & C_4 & D_4 & E_4 \\ A_5 & B_5 & C_5 & D_5 & E_5 \end{vmatrix} \begin{vmatrix} GF/L \\ FE/L \\ y_*/L \\ L_*/L \\ P/L \end{vmatrix} = \begin{vmatrix} F_1 \\ F_2 \\ F_3 \\ F_4 \\ F_5 \end{vmatrix} \qquad (11)$$

where the coefficients (A–F) are obvious from the previous equations. The solution of the matrix requires, for a given (M_1, β) combination, specification of a triple-point solution as well as a value for the height of the wedge trailing edge above the centerline y_t/L.

By assuming all control surfaces and discontinuities to be set a priori by the given upstream conditions, any downstream disturbances that might affect the solution for Mach shock height are ignored. However, "upstream influence" is a concern for certain combinations of wedge geometry and freestream conditions. It seems that any disturbances can only propagate upstream via the subsonic region, which implies either that region 4 becomes unchoked or that some disturbance is communicated to region 4 upstream of the sonic line. Previous investigators[13,18] have observed that the trailing-edge expansion plays a role in the upstream displacement of the Mach stem. It is clear that the mechanism must be related to some rise in the downstream pressure—the Mach stem is displaced to satisfy flow rate continuity in the duct.

The authors suggest here that the high downstream pressure is caused by the pressure rise across a shock (i.e., the reflected shock joined to the confluence point T in Fig. 6) impinging on the wedge surface, which acknowledges the wedge length as an important parameter. The rise in static pressure would then be communicated along characteristic lines to some flowfield location close to, and probably downstream of, the sonic line in region 4. (The high pressure could, alternatively, be communicated upstream via the viscous shear layer, if the local shear-layer velocities are subsonic.) Thus it is probable that this back pressure would simply displace the Mach stem. Unfortunately, it was not possible to quantify, or even validate, this mechanism with the data from the tests by Hornung and Robinson made available to these authors. However, the data do suggest that only the scale of the shock system is altered when the Mach stem moves upstream and not the geometric relations among the various discontinuities.

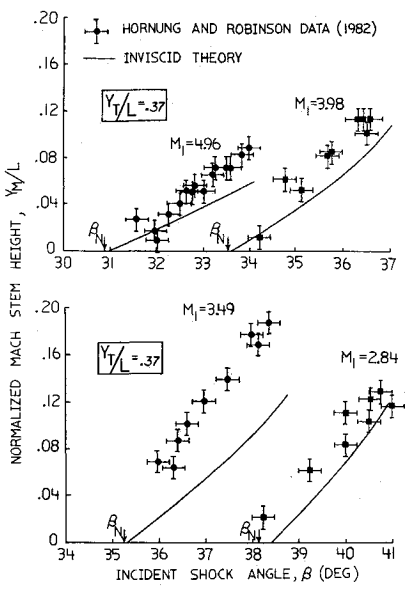

Fig. 7 Comparison of predicted Mach stem heights and the unpublished experimental data of Hornung and Robinson.[10]

Table 1 Sensitivity of stem height to uncertainty in freestream Mach number (y_t/L = 0.37)

β, deg	y_M/L	y_M/L	Difference, %
	M_1 = 2.80	M_1 = 2.84	
38.90	0.0204	0.0290	42.2
39.40	0.0431	0.0516	19.7
39.90	0.0670	0.0751	12.1
40.40	0.0915	0.0999	9.2
40.90	0.1171	0.1254	7.1
41.40	0.1436	0.1527	6.3
	M_1 = 4.93	M_1 = 5.00	
31.50	0.0068	0.0062	9.7
32.50	0.0240	0.0262	9.2
33.50	0.0436	0.0456	4.6
34.50	0.0659	0.0678	2.9
35.50	0.0913	0.0932	2.1
	M_1 = 9.86	M_1 = 10.00	
25.40	0.0000	0.0001	—
26.40	0.0030	0.0030	0.0
27.40	0.0072	0.0072	0.0
28.40	0.0127	0.0128	0.0
29.40	0.0199	0.0199	0.0

Results

This discussion will be presented in two sections. The entire flow will be treated as inviscid, and predictions from Eq. (11) will be compared with certain unpublished experimental data of Hornung and Robinson.[10]

A comparison between the predictions based on the control-volume approach and Hornung and Robinson's data for a similar two-dimensional wedge geometry is given in Fig. 7. Those investigators oriented two wedges symmetrically about a centerline in a blowdown wind tunnel (see Fig. 2b). Schlieren and shadowgraph photos were taken of the steady-flow shock patterns that developed as the angle of incidence β was gradually increased. The pivot point of the wedges was such that the distance between the trailing edges was kept almost constant with shock angle, for the range of shock angles examined. The uncertainty associated with measuring Mach stem height and β from the optical records is provided in Fig. 7.

The predicted values are lower than the experimental data, for all freestream Mach numbers examined, even when allowance is made for the measurement uncertainty in y_M and β. However, the computed β_N value is accurate to within a fraction of a degree. It does seem, then, that the assumptions employed in the model are plausible and that the model is, at least for these test conditions, a reasonable first approximation. The following discussion considers the relative sensitivity of the predicted Mach stem heights to experimental uncertainties not shown in Fig. 7 as well as to the various assumptions employed in the model.

Although the direct measurement uncertainty in y_M and β has been shown, there is an additional uncertainty in y_M associated with both the y_t measurement and the freestream Mach number determination. Tables 1 and 2 illustrate, respectively, each of these two effects. The $M_1 = 10$ situation is provided only to show how the y_M sensitivity might be extrapolated to higher Mach numbers.

The ratio y_t/L was 0.37 for all of the test conditions shown in Fig. 7, a value measured from the photographs and thus subject to the same uncertainty as previously given for y_M/L, that is, ± 0.01 (i.e., $0.36 \leq y_t/L \leq 0.38$). The M_1 uncertainty is $\pm 0.5\%$ according to Ref. 10. It is seen in Table 2 that, in the range $M_1 \leq 5$, the uncertainty in y_t contributes only slightly to the experimental y_M uncertainty shown in Fig. 7. The sensi-

Table 2 Sensitivity of stem height to uncertainty in the trailing-edge height y_t/L

M_1	β, deg	$\frac{y_M}{L}\left(\frac{y_t}{L}=0.36\right)$	$\frac{y_M}{L}\left(\frac{y_t}{L}=0.37\right)$	Difference, %
2.80	38.90	0.0206	0.0204	1.0
	39.40	0.0435	0.0431	0.9
	39.90	0.0677	0.0670	1.0
	40.40	0.0926	0.0915	1.2
	40.90	0.1184	0.1171	1.1
	41.40	0.1453	0.1436	1.2
5.00	31.00	0.0012	0.0012	0.0
	32.00	0.0179	0.0173	3.5
	33.00	0.0366	0.0356	2.8
	34.00	0.0580	0.0564	2.8
	35.00	0.0823	0.0800	2.9
	36.00	0.1104	0.1074	2.8
	37.00	0.1424	0.1386	2.7
10.00	25.40	0.0001	0.0001	0.0
	26.40	0.0035	0.0030	16.7
	27.40	0.0081	0.0072	12.5
	28.40	0.0142	0.0128	10.9
	29.40	0.0218	0.0199	9.5
	30.40	0.0315	0.0290	8.6
	31.40	0.0432	0.0401	7.7

Table 3 Comparison of predicted slipstream angle ϵ with that obtained from the triple-point solution, $\epsilon_{tp}(y_t/L = 0.37)$

		$p_3 = p_{4avg}$		
M_1	β, deg	y_M/L	ϵ_{tp}, deg	ϵ,[a] deg
2.80	38.90	0.020	0.782	0.691
	39.90	0.067	2.395	2.085
	40.90	0.117	3.978	3.484
	41.90	0.172	5.534	4.861
	42.90	0.231	7.063	6.214
5.00	31.00	0.001	0.115	0.115
	32.00	0.017	1.564	1.514
	33.00	0.036	2.980	2.886
	34.00	0.056	4.368	4.235
	35.00	0.080	5.730	5.565
	36.00	0.107	7.070	6.872
	37.00	0.139	8.387	8.159
10.00	25.40	0.000	0.046	0.045
	26.40	0.003	1.259	1.244
	27.40	0.072	2.449	2.419
	28.40	0.013	3.621	3.579
	29.40	0.020	4.788	4.735
	30.40	0.029	5.940	5.874
	31.40	0.040	7.084	7.013

[a]From Eq. (12).

tivity of y_M to M_1 is higher, and it seems that the lower Mach number data are affected to a larger degree than are the higher Mach number data, the sensitivity at a given Mach number decreasing as $\beta - \beta_N$ increases. The higher sensitivity to M_1 at the lower M_1 values is due to the increased sensitivity of the triple-point solution to M_1 at low Mach numbers.

As β_N decreases (that is, as M_1 is increased from 2.84 to 4.96 to 10.0), the higher flow rates are passed with relatively smaller y_M values. This is why y_M/L increases as M_1 is increased for a given β_N value (β_N is about the same for a $\pm$ 0.5% change in M_1) but decreases as M_1 is raised from 2.84 to 4.96.

Taking into account the aforementioned experimental uncertainties, however, the predictions are still somewhat low. One aspect of the tests that cannot be quantitatively evaluated is the degree of planar flow. According to Hornung and Robinson, the flow is two-dimensional over the central third of the model span.[10] The effect of a mass efflux through the sides of the duct would probably be to lower the stem heights. Thus, a true two-dimensional flow may produce higher Mach stem heights than those presented in Fig. 7, resulting in a larger disagreement with the inviscid predictions. However, the three-dimensional flow over the other two-thirds of the span may also have influenced the optical data records from which many of the geometric measurements were taken.

We will now evaluate the sensitivity of y_M to the various model assumptions. The three assumptions to be considered are 1) the accuracy of the triple-point solution, 2) the representation of the Mach stem as a normal shock wave, and 3) the degree to which slipstream curvature can be ignored.

The triple-point solutions were obtained by an iterative solution of the Rankine-Hugoniot equations with the requirement that the static pressure on both sides of the slipstream is the same (i.e., $p_{4avg}/p_3 = 1$). Iteration on the slipstream angle was performed until this pressure ratio was achieved to within $\pm$ 1.0%, as this degree of accuracy resulted in reasonable convergence times on a VAX Cluster mainframe. The accuracy was improved to $\pm$ 0.1% for selected upstream conditions to determine whether the y_M predictions would be measurably improved. The result of the improved computation was that y_M values shown in Fig. 7 were increased by about 5-10% for angles close to the von Neumann angle for all Mach numbers. This increase only partially recovers, by itself, the observed discrepancies between theory and experiment.

Evaluation of the available photographic data verified that the reflected shock wave in all cases was straight, with an angle predicted by the triple-point solution. Likewise, the Mach stem was observed to be normal to the upstream flow over the physical distance resolvable by the data acquisition equipment. To examine whether deviation from this is present at the triple point and whether such deviation would alter the y_M predictions, the triple-point solution algorithm was altered so that the angle of the Mach stem, in addition to the slipstream angle, was iterated upon. The result of this was that the stem heights determined assuming a normal Mach stem agreed to within less than 1% with those calculated using an oblique Mach stem at the confluence T. This shows, then, that a normal Mach stem assumption is valid for the length-scale predictions.

Since slipstream angles could not be measured accurately from the optical records, values were computed from the predicted y_M and y_* values, assuming the slipstream to be straight:

$$\tan \epsilon = \frac{y_M - y_*}{L_*} \tag{12}$$

A comparison between these predicted slipstream angles and the triple-point solutions (ϵ_{tp}) is given in Table 3. It appears that the two angles agree better at higher Mach numbers, with only a minor β dependence (of $\epsilon_{tp} - \epsilon$) observed, suggesting that the straight slipstream assumption improves as the Mach number increases, or at least that the "effective" slipstream angle approaches that of the triple-point solution as Mach number increases.

To summarize the discussion to this point, it can be said that the control-volume approach, as applied here, can produce the desired length-scale information. The computed Mach stem heights were found to be less than those measured from Hornung and Robinson's experimental data, and the discrepancies are recovered partially by considering experimental uncertainties. The sensitivity of the Mach stem heights to the various assumptions of the model was also investigated. Although it appears that no single assumption controls y_M to any large degree, the combined effect recovers most of the difference between this simple theory and experiment.

Summary

The previous discussion has centered on a predictive scheme for Mach stem heights associated with steady-flow Mach reflection using the results of von Neumann's three-shock the-

ory. High-speed flows were of particular interest because of the current interest in supersonic diffusers for scramjet applications. The two-dimensional wedge-bounded situation was investigated because of its simplicity and the availability of relevant experimental data.

By introducing certain assumptions, primarily that of straight shocks and a one-dimensional flow approximation for the embedded subsonic region, a control-volume analysis became possible. The resultant algebraic equations were solved to determine a unique Mach reflection shock pattern. Subsequent analysis of the predictions showed that the inviscid calculations agree well with certain test data acquired by others. Discrepancies between the present model and empirical results can be almost completely recovered by accounting for experimental uncertainties as well as the sensitivity of the theoretical results to certain assumptions of the model.

A mechanism by which the trailing-edge expansion fan can displace the Mach stem upstream was suggested. This "upstream influence" noted by previous investigators has never been explored quantitatively for the present situation. No validation of this mechanism was possible with the data made available to the present authors. The wedge length would be an important parameter in any such analysis, and it appears that an iterative procedure would be required for any prediction of the resultant shock structure. Furthermore, it appears that the rise in downstream pressure suggested as causing the upstream influence serves only to increase the scale of the shock pattern.

It is believed that the model presented identifies the dominant influences affecting the scale of the shock pattern in certain steady-flow situations. The work was intended to complement the relatively large effort devoted, historically, to pseudosteady and unsteady wedge-type flows, as well as to provide a basis for a more complete steady-flow model. Although comparable computational fluid dynamics results are not included here, it would be interesting to compare conventional Euler calculations with the analytical approach developed in this paper.

Acknowledgments

Our thanks go to William J. Rae, who provided timely financial aid throughout this research via NASA Hypersonics Grant NAGW-966. The authors also express their sincere appreciation to Hans Hornung of the California Institute of Technology, who graciously allowed access to his unpublished experimental data.

References

[1]Goldberg, T. J., and Hefner, J. N., "Starting Phenomena for Hypersonic Inlets with Thick Turbulent Boundary Layers at Mach 6," NASA TN-D-6280, Aug. 1971.

[2]Azevedo, D. J., Liu, C. S., and Rae, W. J., "Prediction of Inviscid Stagnation Pressure Losses in Bounded High-Speed Flows," *AIAA Journal,* Vol. 28, No. 10, 1990, pp. 1834–1836.

[3]Nagamatsu, H. T., and Horvay, G., "Supersonic Jet Noise," AIAA Paper 70-237, 1970.

[4]Edney, B. E., "Anomalous Heat Transfer and Pressure Distributions on Blunt Bodies at Hypersonic Speeds in the Presence of an Impinging Shock," Aeronautical Research Inst. of Sweden, FFA Rept. 115, Stockholm, 1968.

[5]Von Neumann, J., "Oblique Reflection of Shocks," Navy Dept. (Bureau of Ordnance), Explosives Research Rept. 12, 1943; (also *Collected Works,* Vol. 6, Pergamon Press, Oxford, England, UK, pp. 238–299).

[6]Henderson, L. F., and Lozzi, A., "Experiments on Transition of Mach Reflexion," *Journal of Fluid Mechanics,* Vol. 68, Pt. 1, 1975, pp. 139–155.

[7]Ben-Dor, G., "Steady, Pseudo-Steady and Unsteady Shock Wave Reflections," *Progress in Aerospace Science,* Vol. 25, 1988, p. 387.

[8]Courant, R., and Friedrichs, K. O., *Supersonic Flow and Shock Waves,* Springer-Verlag, New York, 1948, p. 341.

[9]Henderson, L. F., and Lozzi, A., "Further Experiments on Transition to Mach Reflexion," *Journal of Fluid Mechanics,* Vol. 94, Pt. 3, 1979, pp. 541–559.

[10]Hornung, H. G., and Robinson, M. L., "Transition from Regular to Mach Reflection of Shock Waves, Part 2: The Steady-Flow Criterion," *Journal of Fluid Mechanics,* Vol. 123, 1982, pp. 155–164.

[11]Hornung, H. G., "Regular and Mach Reflection of Shock Waves," *Annual Review of Fluid Mechanics,* Vol. 18, 1986, pp. 33–58.

[12]Curle, N., and Davies, H. J., *Modern Fluid Dynamics,* Vol. II, Van Nostrand, London, England, UK, 1971, pp. 133,134.

[13]Sternberg, J., "Triple Shock-Wave Intersections," *Physics of Fluids,* Vol. 2, No. 2, 1959, pp. 178–206.

[14]Chow, W. L., and Addy, A. L., "Interaction Between Primary and Secondary Streams of Supersonic Ejector Systems and Their Performance Characteristics," *AIAA Journal,* Vol. 2, No. 4, 1964, pp. 686–695.

[15]Back, L. H., and Cuffel, R. F., "Viscous Slipstream Flow Downstream of a Centerline Mach Reflection," *AIAA Journal,* Vol. 9, No. 10, 1971, pp. 2107–2109.

[16]Skews, B. W., "The Flow in the Vicinity of a Three-Shock Intersection," *Canadian Aeronautics and Space Institute Transactions,* Vol. 4, No. 2, 1971, pp. 99–107.

[17]Ben-Dor, F., "A Reconsideration of the Three-Shock Theory for a Pseudo-Steady Mach Reflection," *Journal of Fluid Mechanics,* Vol. 181, 1987, pp. 467–484.

[18]Holden, M. S., Wieting, A. R., Moselle, J. C., and Glass, C., "Studies of Aerothermal Loads Generated in Regions of Shock/Shock Interaction in Hypersonic Flow," AIAA Paper 88-0477, Jan. 1988.